IL NUOVO CIMENTO **39 C** (2016) 274
DOI 10.1393/ncc/i2016-16274-1

COMMUNICATIONS: SIF Congress 2015

Search for dark matter at LHC

M. CIPRIANI([1])([2])([*])

([1]) *INFN, Sezione di Roma - Roma, Italy*
([2]) *Dipartimento di Fisica, Università di Roma "La Sapienza" - Roma, Italy*

received 1 February 2016

Summary. — The existence of dark matter in our universe is supported by many astrophysical observations and is one of the most compelling hints of new physics beyond the Standard Model, although there is not yet any direct evidence of dark-matter particles. The Large Hadron Collider (LHC) represents a powerful tool that can potentially discover dark matter through its direct production in proton-proton collisions. The aim of this article is to present the search for dark matter candidates in events with large missing transverse energy and one or more high energy jets collected with the CMS detector at LHC. Results obtained during Run1 with the 8 TeV data and their interpretation are reported. In addition, prospects for the 13 TeV analysis during Run2 and the discovery potential are also discussed.

1. – Introduction

The existence of dark matter (DM) in our universe is supported by many astrophysical observations [1]. Evidence for DM is established from its gravitational effects on visible matter, yet the Standard Model (SM) of particle physics does not provide any candidate to explain its presence. For this reason, DM represents one of the most compelling hints for the existence of new physics beyond the SM.

The DM candidates are assumed to be weakly interacting massive particles (WIMP) which are not subject to strong and electromagnetic interactions. At the LHC, they can be produced in pairs through a contact interaction or the exchange of a heavy mediator.

The search for DM at colliders is complementary to searches for annihilation of DM to SM particles [2] (indirect searches) or DM scattering on nuclei [3] (direct searches). Their experimental sensitivity is different and depends on m_{DM} (DM candidate mass) and the specific Lorentz structure of the interaction (vectorial, axial, scalar, pseudoscalar).

A simple approach to describe the interaction of DM with SM particles is to exploit an effective field theory (EFT) in which a contact interaction involving partons and DM

([*]) E-mail: marco.cipriani@uniroma1.it, marco.cipriani@roma1.infn.it

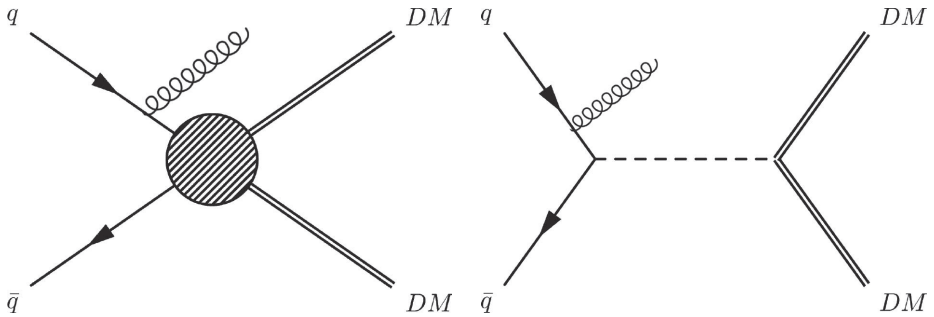

Fig. 1. – Feynman diagrams showing production of dark matter through a contact interaction (left) or the exchange of a mediator (right). Radiation from the initial state is used to tag and trigger the event.

is assumed [4, 5]. In this way, the interaction is characterized by m_{DM}, a mass scale M_* related to the energy scale (roughly ranging from few to tens of TeV) above which the EFT assumption is no more valid, and the Lorentz coupling structure. The EFT approach was the baseline for the interpretation of results obtained with data collected by LHC with a centre-of-mass energy of 8 TeV up to 2012 (this phase being called Run1).

The EFT model leads to several limitations: first of all, it is assumed that the effective scale M_* is not accessible at the available centre-of-mass energy, which means that a possible mediator is so heavy that it cannot be resonantly produced; secondly, unitarity would be violated for low enough M_*; thirdly, a comparison with direct detection experiment is inconsistent due to the incompleteness of the EFT model.

With the increase of the centre-of-mass energy from 8 to 13 TeV after the LHC restart in 2015 (and the beginning of the new data taking period referred to as Run2), the EFT approach might not be valid and a more accurate interpretation of results is obtained with the so-called "simplified models", taking into account the resonant production of a mediator. This adds other free parameters such as the mediator mass m_{med} and the coupling constants, g_{SM} and g_{DM}, between the mediator and the partons or the DM. Benchmarks for the interpretation of DM collider search results in terms of simplified models were organized by the Dark Matter Forum [6]. Figure 1 shows the Feynman diagrams for the production of DM through a contact interaction (fig. 1(a)) or the exchange of a mediator (fig. 1(b)).

Since DM is assumed to be weakly interacting and neutral, it would not produce any discernible signal in the detector. For this reason, signal events are required to include other detectable particles coming from initial-state radiation (ISR) from the incoming particles, which might be a photon, a weak boson or a jet (a bunch of particles produced as a consequence of gluon or quark hadronization). The latter case is the one considered in this paper and such events are referred to as monojet, for which the jet is exploited to tag and trigger the event.

Although DM is not directly detected, its presence can be inferred from an imbalance in the vector sum of the momenta of all reconstructed particles in the transverse plane, orthogonal to the beam axis. The magnitude of a particle's transverse momentum is denoted by p_{T}. Since the beams have no momentum component along the transverse plane, the total transverse momentum must be zero because of momentum conservation. The

magnitude of the imbalance, computed as the negative vector sum of all reconstructed particles' momenta, is called missing transverse energy and is denoted by $E_{\mathrm{T}}^{\mathrm{miss}}$. Monojet events are thus characterized by the presence of at least one high p_{T} jet (additional jets might be emitted as further radiation from the colliding partons) recoiling against DM particles, *e.g.* $E_{\mathrm{T}}^{\mathrm{miss}}$.

The monojet analysis [7-9] is the most sensitive among all the ones involving the radiation of a SM particle from the initial state (generically denoted mono-X searches), since the cross-section for the emission of a strongly interacting particle is higher than that of an electroweakly interacting one. Nevertheless, all other mono-X searches are also important as cross-checks to the monojet signature: indeed, in case a signal is observed in the monojet channel, then it should also appear in the other channels provided that enough data are collected in order to compensate for the lower cross-section.

2. – CMS detector

The Compact Muon Solenoid (CMS), described with more details in ref. [10], is a multi-purpose detector designed to detect and measure the properties of all particles produced in proton-proton or heavy-ion collisions.

The CMS apparatus features a superconducting solenoid which provides a magnetic field of 3.8 T parallel to the beam line. Inside it there are: the tracker, which is used to measure charged particles' momentum through the curvature of their trajectories bent by the magnetic field; the crystal electromagnetic calorimeter, which measures the energy of photons and electrons; the hadronic calorimeter, where hadrons deposit their energy. Muon detectors are placed outside the solenoid, embedded in the steel flux return yoke. In combination with the inner tracker, they allow for a precise measurement of muons' momentum.

Offline, particle candidates are reconstructed with a particle-flow algorithm [11], which exploits basic information from all detectors to build more complex objects (for instance, tracks or energy clusters) used to identify charged or neutral hadrons, photons, muons or electrons.

The direction of each reconstructed particle is described by two angular variables: the angle ϕ in the transverse plane and the pseudorapidity η ($\eta = -\ln \mathrm{tg}\ (\theta/2)$, where θ is the angle with respect to the beam line).

3. – Event selection

The main backgrounds for the monojet search are made of: $Z(\nu\nu)+$jets events, where the Z boson decays to neutrinos; $\mathrm{W}(l\nu)$ + jets, where the W decays to a charged lepton (electron, muon or tau) and a neutrino. Neutrinos only interact weakly and thus escape detection producing genuine $E_{\mathrm{T}}^{\mathrm{miss}}$, while the charged lepton from the W might fall outside the detector acceptance region or in a poorly instrumented region, or simply it might not be detected due to detector inefficiencies. These background processes are indistinguishable from the signal and are thus irreducible. After the full event selection described later, these processes constitute about 95% of the total background. Other reducible backgrounds consist of: top quark production ($t\bar{t}$ or single top), diboson production (ZZ, ZW and WW), Quantum Chromodynamics (QCD) events with many jets produced, $\mathrm{Z}(ll)+$jets with the Z decaying to charged leptons. Such processes are distinguishable from the signal since they generally have charged leptons, high jet multiplicity or no $E_{\mathrm{T}}^{\mathrm{miss}}$ (unless neutrinos are produced, although fake $E_{\mathrm{T}}^{\mathrm{miss}}$ can potentially be present

if one or more particles are undetected or their energy is not measured correctly) and consequently they can be suppressed by rejecting events which contain leptons or have low values of measured $E_{\mathrm{T}}^{\mathrm{miss}}$.

The main observable for this analysis is the $E_{\mathrm{T}}^{\mathrm{miss}}$ distribution. A possible signal would appear as an excess of events in the high $E_{\mathrm{T}}^{\mathrm{miss}}$ region and can be extracted through two different strategies: the "cut-and-count" analysis consists in counting the number of events above a given (relatively high) $E_{\mathrm{T}}^{\mathrm{miss}}$ threshold and looking for an excess with respect to the expected background yield; in the "shape analysis" the signal is extracted through a maximum-likelihood fit to the $E_{\mathrm{T}}^{\mathrm{miss}}$ distribution. The shape analysis generally provides a better sensitivity with respect to the cut-and-count one, because it is sensitive to signal events located in all the $E_{\mathrm{T}}^{\mathrm{miss}}$ distribution and not just those in the high $E_{\mathrm{T}}^{\mathrm{miss}}$ region.

Signal events are required to satisfy a number of selection criteria to reduce the background component. Those described in this section refer to the 8 TeV analysis [7]. The 13 TeV preliminary results, presented at the end of December 2015 [9], are mainly based on the 8 TeV analysis described in ref. [8], but updated selection criteria are adopted.

Events must have $E_{\mathrm{T}}^{\mathrm{miss}} > 200\,\mathrm{GeV}$ and the jet with the highest p_{T} is required to have $p_{\mathrm{T}} > 110\,\mathrm{GeV}$ and $|\eta| < 2.4$. A second jet in the event is allowed if it has $p_{\mathrm{T}} > 30\,\mathrm{GeV}$ and $|\eta| < 4.5$, as long as the angular separation between the two jets satisfies $\Delta\phi < 2.5$. The latter condition aims at suppressing typical QCD dijet events where two jets are produced back-to-back in the transverse plane. Events with more than two jets are rejected to further suppress QCD or top quarks events leading to final states with many jets. Finally, all events with reconstructed photons or charged leptons are rejected. This last requirement reduces the contamination from events with Z/W bosons or top quarks decaying to charged leptons.

4. – Background estimate

The cross-section for DM production is expected to be several order of magnitude lower than that for background processes. Therefore, a precise determination of the background $E_{\mathrm{T}}^{\mathrm{miss}}$ distribution is necessary to assess the observation of a possible signal. For the cut-and-count analysis only the backgrounds' normalization is needed.

Reducible backgrounds are small and are estimated from Monte Carlo (MC) simulation. Irreducible backgrounds are estimated in a data-driven way. The $E_{\mathrm{T}}^{\mathrm{miss}}$ distribution and its normalization are obtained from data control regions and is used to predict the $E_{\mathrm{T}}^{\mathrm{miss}}$ shape of the background process in the signal region through scale factors computed from simulations. In other words, the number of background events expected in the signal region should be equal to the number of events in a control region after correcting for the different cross-section and selection efficiency: such corrections are accounted for by the MC scale factors.

The Z($\nu\nu$)+jets background is estimated through a Z($\mu\mu$)+jets control sample. The two processes are identical as far as kinematics is concerned, the only difference lying in the different Z boson's decay branching ratio and in the different acceptance and selection efficiency for the two processes (another difference would be the fact that muons can also couple to photons, but this effect is negligible since the invariant mass of the two muons is required to be in an interval centred at the nominal Z mass). However, the Z branching ratios are such that the number of Z bosons decaying to muons is about six times smaller than the number of decays to neutrinos, and therefore the statistical uncertainty on

the number of $Z(\mu\mu)$ + jets events becomes an important systematic uncertainty on the predicted yield for $Z(\nu\nu)$ + jets events, especially in the high E_T^{miss} region.

For this reason, a γ + jets control sample is used as well to further constrain the $Z(\nu\nu)$ + jets prediction. This sample is similar to the $Z(\mu\mu)$ + jets one after substituting the Z boson with a photon, but has a higher cross-section and thus provides higher statistics. Nevertheless, this prediction relies on the theoretical knowledge of the ratio between $Z(\nu\nu)$ + jets and γ + jets cross-sections, adding another source of systematic uncertainty. The $W(l\nu)$ + jets background is estimated using a $W(\mu\nu)$ + jets sample.

It has to be noted that there is no genuine E_T^{miss} in the control processes (apart from the $W(\mu\nu)$ + jets sample, where neutrinos are produced) and thus, in order to link these samples to the background to be predicted, a fake E_T^{miss} is defined by excluding the muons (for the $Z(\mu\mu)$ + jets and $W(\mu\nu)$ + jets samples) or the photon (for the γ + jets sample) from the event. Taking the $Z(\mu\mu)$ + jets as an example, this implies that, neglecting other sources of E_T^{miss} coming from bad reconstruction issues, the fake E_T^{miss} distribution is roughly equal to the Z boson's p_T.

5. – Performance of E_T^{miss} reconstruction

As outlined before, it is extremely important to measure the E_T^{miss} with the best possible precision. The E_T^{miss} reconstruction performance is assessed by studying the experimental resolution and response (or scale) on the E_T^{miss} [12] which, for signal-like events, is basically the opposite of the hadronic recoil (*e.g.* the negative vector sum of jets' p_T). Hence, the largest source of uncertainty on the E_T^{miss} measurement comes from the jet energy resolution. This study is conducted using $Z(ll)$ + jets, with a Z boson decaying either to electrons or muons, and γ + jets samples.

As for the control regions, these events have no real E_T^{miss} since ideally the boson's and the jets' p_T are perfectly balanced: in fact they are not because of detector inefficiencies, particles' momentum mismeasurements or other physics effects such as the energy contribution from pile-up interactions. The pile-up is the overlap of multiple proton interactions that can occur when two proton bunches collide (moreover, there can be a contamination from energy deposited by particles produced in earlier or later bunch crossings).

A fake E_T^{miss} is thus defined as the boson's p_T. Moreover, since the resolution on the boson's p_T is much better than that on jets' energy, it is possible to use the Z/γ as a reference to compare the measurement of the recoil. In particular, the two projections of the recoil along and orthogonal to the boson's p_T direction (denoted as $u_\parallel$ and $u_\perp$ respectively) are considered: the resolution is defined for each projection as the standard deviation of their distributions, which are approximately Gaussian, and are evaluated both as a function of the boson's p_T and the number of reconstructed vertices; the response is defined as the mean value of the distribution of the ratio between $u_\parallel$ and the boson's p_T (which should be equal to unity for perfectly balanced events) and is computed as a function of the boson's p_T to get the response curve.

Studies with 8 TeV data showed a good agreement between data and MC, while some discrepancies were found with preliminary 13 TeV data. Such discrepancies pointed to some calibration issues related mostly to a miscalibration of the response of the forward hadron calorimeter. After correcting for these effects, a good agreement was found for 13 TeV data as well.

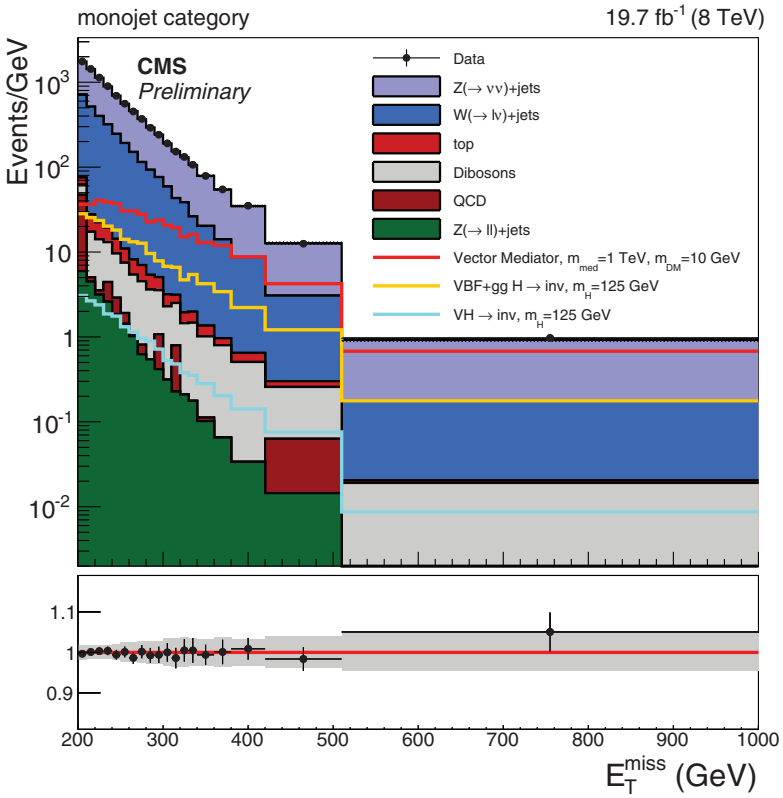

Fig. 2. – Distribution of $E_{\mathrm{T}}^{\mathrm{miss}}$ expected from SM backgrounds (filled stacked histograms) and observed in data (black dots) in the signal region. The lower panel shows the data/background ratio and the grey band indicates the uncertainty on the background prediction. Figure taken from [8].

6. – Results and perspectives

The total dataset used for the 8 TeV analysis corresponds to an integrated luminosity of $19.7\,\mathrm{fb}^{-1}$ ($1\mathrm{b} = 10^{-24}\,\mathrm{cm}^2$ and the expected number of events is given by the product of its cross-section and the integrated luminosity). The signal is extracted through a maximum likelihood fit to the expected $E_{\mathrm{T}}^{\mathrm{miss}}$ distribution from all backgrounds in the signal region. The $E_{\mathrm{T}}^{\mathrm{miss}}$ distribution is shown for both data and estimated background in fig. 2. The main backgrounds are predicted from control regions. Data are consistent with the background yields and agreement at the percent level is observed in all $E_{\mathrm{T}}^{\mathrm{miss}}$ intervals. Therefore, upper limits are set on the cross-section for DM production.

It has to be noted that limits on the cross-section depend on several parameters such as the DM mass, the mediator's mass, couplings to SM and DM particles and the Lorentz coupling structure of the interaction. In fig. 3, the 90% CL exclusion contours for the spin-independent production cross section as a function of the DM mass are shown, under the hypothesis of a vector interaction through the exchange of a heavy mediator. For the sake of comparison with direct detection experiments, the figure also shows the limit set by the LUX experiment, which provides the strongest bounds for $m_{\mathrm{DM}} > 6\,\mathrm{GeV}$. It

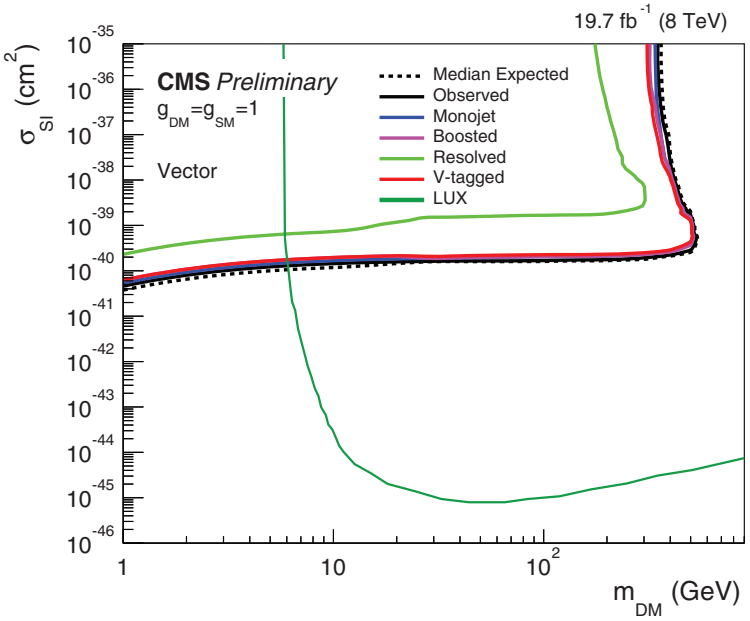

Fig. 3. – The figure shows 90% CL exclusion contours in the $m_{\rm DM}$-$\sigma_{\rm SI}$ plane (dark matter mass and spin-indipendent cross-section) under the assumption of a vector mediator, with $g_{\rm DM}$ and $g_{\rm SM}$ couplings to dark matter and quarks, respectively. The monojet limit lies around $10^{-40}\,\mathrm{cm}^2$ and the excluded region is to the top left of the contour. Categories other than monojet refer to the mono-Z/W analysis, which is not discussed in this paper (for further details, see [8]). The lowest line represents the limit set by the LUX experiment [6].

is interesting to note the complementarity between DM searches at colliders and direct searches, highlighted by the fact that the former can explore lower DM mass regions where the latter would have little or no sensitivity at all.

Concerning the Run2 analysis with data collected with a centre-of-mass energy of 13 TeV, the analysis strategy is similar to that at 8 TeV, with many improvements including: the addition of control samples with electrons (*e.g.*, Z(ee)+jets and W($e\nu$)+jets) to further constrain the two irreducible backgrounds; the use of the W($l\nu$) + jets samples to constrain the Z($\nu\nu$)+jets background in a similar way as already done with the γ+jets sample; the selection optimization to enhance the analysis sensitivity; finally, a better estimate of the QCD background with a data-driven approach in order to model the shape of the QCD high $E_{\rm T}^{\rm miss}$ region with the best possible accuracy. In fact, although the QCD background is expected to be negligible after the selection, the large uncertainty on the QCD high $E_{\rm T}^{\rm miss}$ tail prediction might potentially contribute to hide a possible signal, given the huge QCD events' s cross-section compared to the signal's one.

More data at 13 TeV are needed to be competitive with the Run1 results. However, the analysis sensitivity is expected to be enhanced by roughly four times thanks to the higher energy of the collisions, which entails an increase in the production cross-sections. This means that, with just about $5\,\mathrm{fb}^{-1}$ of data, it will be possible to set the same limits as in Run1 and therefore, by collecting more data, become sensitive to a potential discovery.

REFERENCES

[1] Planck Collaboration, *Planck 2015 results. XIII. Cosmological parameters*, arXiv:1502.01589 and references therein.
[2] Fermi-LAT Collaboration, *Searching for Dark Matter Annihilation from Milky Way Dwarf Spheroidal Galaxies with Six Years of Fermi-LAT Data*, arXiv:1503.02641 and references therein.
[3] LUX Collaboration, *Phys. Rev. Lett.*, **112** (2014) 091303, arXiv:1310.8214.
[4] Beltran M. *et al.*, *JHEP*, **09** (2010) 037, doi:10.1007/JHEP09(2010)037, arXiv:1002.4137.
[5] Goodman J. *et al.*, *Phys. Rev. D*, **82** (2010) 116010, doi:10.1103/PhysRevD.82.116010, arXiv:1008.1783.
[6] Abercrombie D. *et al.*, *Dark Matter Benchmark Models for Early LHC Run-2 Searches: Report of the ATLAS/CMS Dark Matter Forum*, arXiv:1507.00966 and references therein.
[7] CMS Collaboration, *Eur. Phys. J. C*, **75** (2015) 235, doi:10.1140/epjc/s10052-015-3451-4, arXiv:1408.3583.
[8] CMS Collaboration, *Search for New Physics in the V-jet+MET final state* (2015) CMS Physics Analysis Summary.
[9] CMS Collaboration, *Search for dark matter with jets and missing transverse energy at 13 TeV*, (2015) CMS Physics Analysis Summary and references therein.
[10] CMS Collaboration, *JINST*, **3** (2008) S08004.
[11] CMS Collaboration, *Particle-flow event reconstruction in CMS and performance for Jets, Taus, and* $E_{\mathrm{T}}^{\mathrm{miss}}$, CMS-PAS-PFT-09-001 (2009).
[12] CMS Collaboration, *JINST*, **10** (2015) P02006, doi:10.1088/1748-0221/10/02/P02006, arXiv:1411.0511.